

Chapter 36

Optimal Rain Attenuation Prediction Models for Earth-Space Communication at Ku-Band in North Central Nigeria



K. C. Igwe

Abstract Precipitation adversely affects satellite-earth links operating at frequencies ≥ 10 GHz. This paper evaluates five of the best performing rain attenuation models for earth-space links so as to obtain the optimal models for North Central Nigeria. The models considered are ITU-R P.618-9, Bryant, Simple attenuation, Garcia-Lopez and Svjatogor. Also, three elevation angles were considered: 55° (the look angle of most satellite receivers over the Atlantic Ocean Region (AOR) in Nigeria), 23° (the look angle of receivers over the Indian Ocean Region (IOR)) and 42.5° (the look angle of Nigeria's communication satellite (NIGCOMSAT-1R) over the AOR). 2–4 years of 5-min integration time rainfall data was obtained from the Centre for atmospheric research (CAR), Anyigba, Nigeria. The cumulative distribution of rain attenuation at Ku-band was predicted for circularly polarised signals at different percentages of time of the year. Results obtained showed that the ITU-R P.618, Garcia-Lopez and Bryant models performed optimally in this region with attenuation values ranging from 6 to 19 dB at exceedance time percentage of 0.01% in all the stations.

36.1 Introduction

Amongst the debilitating atmospheric effects on satellite-earth links propagating at higher frequency bands (≥ 10 GHz), attenuation by rain is most deleterious to the system's functionality [1–5]. Therefore, it is important to carefully analyse and quantify the extent of attenuation by rain at the frequency of interest [6].

During rainfall, radio waves propagating through the atmosphere at these high frequencies are either absorbed or scattered, thereby resulting to signal reduction [7]. Scattering may in addition cause interference on the radio paths. In the super high frequency (SHF) band, where the wavelength of the radio wave is longer in comparison with the rain drop size, attenuation by absorption will exceed that by

K. C. Igwe (✉)

Department of Physics, Federal University of Technology, Niger State, Minna, Nigeria
e-mail: k.igwe@futminna.edu.ng

scattering. Conversely, in the extreme high frequency (EHF) band and beyond where the wavelength is shorter than the rain drop dimension, attenuation by scattering will be more pronounced [8].

It is difficult to determine the attenuation of electromagnetic signals due to rain because of the unstable nature of rain. Thus, since drop sizes vary temporally and spatially, they do not have a definite arrangement for rainfall rates [9].

Attenuation induced by rain is an important propagation effect that should not be neglected in satellite system design. For optimal analysis of rain attenuation, it is imperative that the corresponding rain rate is accurately evaluated [10]. Some recent works on rain rate attest to this deduction [11–14]. Satellite beacon signals and radiometers are often used to measure rain-induced attenuation but such measurements are done only in very few locations of the world and thus impossible to directly apply the obtained results to all locations. Consequently, in order to make inputs for system margin calculations to be available in every region of the world, meteorological data have been obtained and different rain attenuation models have been developed [15].

In Nigeria, NIGCOMSAT-1R operates on Ku and Ka bands. It is therefore important to know the extent of rain-induced attenuation on satellite-earth links in various locations so as to guide satellite system designers on enhancing the quality of local network contents [16].

This paper therefore evaluates the degree of attenuation induced by rain on satellite-earth communication and further investigates the optimal rain attenuation prediction models in North Central Nigeria by using rainfall data of 5-min integration time as against daily rainfall data used in [16].

36.2 Background

36.2.1 Rainfall Rate Model

Lavergnat-Gole model. The application of this model is given in [17]. It converts cumulative distribution of rain rate from integration time t_1 , to the desired integration time t_2 . This is done by using a conversion factor given as the ratio of the integration times:

$$P_2(R_2) = CF^a P_1(R_1) \quad (36.1)$$

where

$$CF = \frac{t_2}{t_1} \quad (36.2)$$

and

$$R_2 = R_1 / C F^a \quad (36.3)$$

P_1 and P_2 are the cumulative probabilities obtained with rain gauges of t_1 (min) and t_2 (min) integration times respectively, while R_1 (mm/h) and R_2 (mm/h) are the rain rates for P_1 and P_2 respectively.

Parameter 'a' depends on the region of interest. For the temperate region, it is 0.115 [18], while a value of 0.143 was deduced by [19] for the tropical climatic region. This model was used for the rain rate computation since it has recently been adjudged the optimal rain rate model for the North Central region of Nigeria [20].

36.2.2 Rain Attenuation Models

For the rain attenuation models, five amongst the best performing models were selected for rain attenuation estimation in this work. These are the globally accepted ITU-R P.618-9 [21], Bryant [22], Simple attenuation [23], Garcia-Lopez [24] and Svjatogor models [25]. The ITU-R P.618-9 model is explained in detail here, while the other four models are only defined because of space constraint. Their detailed explanation can be found in [16].

ITU-R P. 618-9 model. Rain rate at 0.01% exceedance is used for rain attenuation prediction in this model. Then an adjustment factor is applied for prediction at other percentage exceedances. The parameters required for the procedures are:

$R_{0.01}$ (mm/h)	point rainfall rate at 0.01% of a year.
h_S (km)	Station height above mean sea level
θ (degrees)	Elevation angle
φ : (degrees)	Latitude of the station
f (GHz)	Frequency

The following steps are required for the computation:

Step 1 Compute the rain height, h_R from ITU-R P. 839-3 [26]:

$$h_R = h_o + 0.36km \quad (36.4)$$

where h_o is 0 °C isotherm height above mean sea level.

Step 2 Determine the slant path length, L_S from:

$$L_S = \frac{h_R - h_S}{\text{Sin}\theta} \quad (36.5)$$

Step 3 Compute the horizontal projection, L_G of slant path length using:

$$L_G = L_S \cos \theta \tag{36.6}$$

Step 4 Input $R_{0.01}$ (mm/h).

Step 5 Calculate the specific attenuation, $\gamma_{R0.01}$ (dB/km) at 0.01% from:

$$\gamma_{R0.01} = k R_{0.01}^\alpha \tag{36.7}$$

where k and α are frequency functions determined from ITU-R P.838-3 [27].

Step 6 Compute the horizontal reduction factor, $r_{h0.01}$ using:

$$r_{h0.01} = \frac{1}{1 + 0.78 \sqrt{\left(\frac{L_G \gamma_{R0.01}}{f}\right) - 0.38[1 - \exp(-2L_G)]}} \tag{36.8}$$

Step 7 Calculate the vertical adjustment factor, $v_{0.01}$ (km):

$$L_R = \frac{L_G r_{0.01}}{\cos \theta}, \text{ for } \rho > \theta \tag{36.9}$$

otherwise,

$$L_R = \frac{H_R - H_S}{\sin \theta}, \text{ for } \rho \leq \theta \tag{36.10}$$

where

$$\rho = \tan^{-1} \left(\frac{H_R - H_S}{L_G r_{h0.01}} \right) \tag{36.11}$$

therefore,

$$v_{0.01} = \frac{1}{1 + \sqrt{\sin \theta} \left[31 \left(1 - \exp \left(-\frac{\theta}{[1+\sigma]} \right) \right) \right] \frac{\sqrt{L_G \gamma_{R0.01}}}{f^2} - 0.45]} \tag{36.12}$$

where $\sigma = 36 - |\varphi|$, for $|\varphi| < 36^\circ$; for $|\varphi| \geq 36^\circ$, $\sigma = 0$

Step 8 The effective path length L_{eff} (km) is calculated from:

$$L_E = L_R v_{0.01} \tag{36.13}$$

Step 9 Compute the predicted rain attenuation at 0.01% of an average year using:

$$A_{0.01} = \gamma_{R0.01} L_E \tag{36.14}$$

Step 10 Obtain the attenuation for other percentage exceedances from:

$$A_p(dB) = A_{0.01} \left(\frac{p}{0.01} \right)^{-[0.655+0.033\ln(p)-0.045\ln(A_{0.01})-z\sin\theta(1-p)]} \quad (36.15)$$

where p is the percentage probability of interest. z is obtained from:

$$z = 0 \text{ if } p \geq 1\% \text{ or } |\varphi| \geq 36^\circ; \quad (36.16)$$

$$z = -0.005(|\varphi| - 36) \text{ if } p < 1\% \text{ and } |\varphi| < 36^\circ \text{ for } \theta \geq 25^\circ; \quad (36.17)$$

else

$$z = -0.005(|\varphi| - 36) + 1.8 - 4.25\sin\theta, \text{ for } \theta < 25^\circ \text{ and } |\varphi| < 36^\circ \quad (36.18)$$

Bryant Model. The Bryant attenuation model uses the ‘effective rain cell’ and ‘variable rain height’ concept to compute rain attenuation.

Simple Attenuation Model. This model also uses point rainfall rate for prediction. As an improvement from an earlier version, the effect of wave polarisation is now incorporated [28]

Garcia-Lopez Model. The Garcia-Lopez attenuation model is an extension of the one proposed for terrestrial links. In this model, separate coefficient values are adopted for tropical regions during computation.

Svjatogor Model. This is a type of rain attenuation model whose effective rain height is a function of the rain intensity.

36.3 Methodology

Rainfall at 5-min integration time was collected at the Tropospheric data acquisition network (TRODAN) located at the mini campus of Federal University of Technology, Minna, Nigeria. This data acquisition station was set up by the Centre for atmospheric research (CAR), Anyigba, Nigeria. Data from four other Universities in the North Central region where the TRODAN weather stations are also situated were used in this work. These are Kogi State University, Anyigba, Benue State University, Makurdi and the Universities of Abuja and Jos. The rainfall data was measured by the Campbell CR-1000 data logger. Figure 36.1 shows the TRODAN weather station.

The Lavergnat and Gole model outlined in Eqs. (36.1)–(36.3) was used to estimate the rainfall rate (mm/h), while the ITU-R P.618-9 outlined in Eqs. (36.4)–(36.18), the Bryant, Garcia-Lopez, Simple attenuation and Svjatogor models were used to predict the rain attenuation. Circular polarisation was considered and the Ku-band downlink centre frequency of 12.675 GHz was used in the analysis. Also, three elevation angles were considered. These are 55° (Look angle of satellite receivers



Fig. 36.1 a The TRODAN weather station (Campbell data logger and solar panel). b Tipping bucket rain gauge

over the AOR in Nigeria), 42.5° (Look angle of NIGCOMSAT-1R over the AOR) and 23° (Look angle of receivers over the IOR).

Table 36.1 lists the input parameters needed for the rain attenuation prediction models.

Table 36.1 Input parameters for the rain attenuation prediction models

Rain model	λ	H_S	θ	f	k, α	$R_p(p)$	$R_{0.01}$
Bryant		✓	✓		✓	✓	
Garcia-Lopez	✓	✓	✓		✓	✓	
ITU-R P.618-9	✓	✓	✓	✓	✓		✓
SAM	✓	✓	✓		✓	✓	
Svjatogor		✓	✓		✓	✓	

where λ : latitude of the station ($^\circ$), H_S : altitude of the station (km), θ : elevation angle ($^\circ$), f: frequency (GHz), k and α : frequency and polarisation dependent coefficients [27], p: time percentage of the year (%), $R_p(p)$: point rainfall rate distribution (mm/h), $R_{0.01}$: point rainfall rate at 0.01% (mm/h)

Table 36.2 Computed rainfall rate at 0.01%

Station	Lat (°N)	Lon (°E)	Altitude (m)	$R_{0.01}$ (mm/h)
Minna	9.54	6.54	249	75.50
Anyigba	7.25	7.18	420	37.80
Makurdi	7.70	8.50	142	75.50
Abuja	9.00	7.28	334	44.00
Jos	9.58	8.57	1110	75.50

36.4 Results and Discussion

36.4.1 Rainfall Rate Estimation

The station characteristics, including the computed rainfall rate $R_{0.01}$ for the North Central region are given in Table 36.2.

36.4.2 Rain Attenuation Prediction

The five predefined models were used to predict rain attenuation at the five stations and comparison of the results were made based on the ITU-R P.618 model. This is because the ITU-R P.618 model has been widely accepted as a very accurate method for estimating rain attenuation on satellite-earth link systems all over the world. When measured data are not available, developed models are usually compared with it [29] since it has been shown that the ITU-R P.618 prediction model agrees closely with measured attenuation values [30–33].

Tables 36.3, 36.4 and 36.5 give values of the relevant input parameters computed using ITU-R P.618-9 model for the three elevation angles.

Figure 36.2a–e show the cumulative distribution of predicted rain attenuation for the stations at 55° elevation angle

From Fig. 36.2, it can be seen that predictions by Bryant and Garcia-Lopez models are close to that of the ITU-R P.618-9 model, though with little deviations of about

Table 36.3 Computed input parameters at 55° elevation angle

Station	h_R (km)	L_S (km)	L_G (km)	L_E (km)
Minna	4.79	5.54	3.18	3.61
Anyigba	4.75	5.28	3.03	5.04
Makurdi	4.76	5.64	3.23	3.68
Abuja	4.76	5.40	3.10	4.72
Jos	4.76	4.45	2.55	3.22

Table 36.4 Computed input parameters at 42.5° elevation angle

Station	h_R (km)	L_S (km)	L_G (km)	L_E (km)
Minna	4.79	6.72	4.95	3.67
Anyigba	4.75	6.41	4.72	5.25
Makurdi	4.76	6.84	5.04	3.75
Abuja	4.76	6.55	4.83	4.89
Jos	4.76	5.40	3.98	3.30

Table 36.5 Computed input parameters at 23° elevation angle

Station	h_R (km)	L_S (km)	L_G (km)	L_E (km)
Minna	4.79	11.61	10.69	5.02
Anyigba	4.75	11.08	10.20	7.22
Makurdi	4.76	11.82	10.88	5.14
Abuja	4.76	11.33	10.43	6.70
Jos	4.76	9.33	8.59	4.51

2–5 dB. It can also be observed that stations that recorded the same rainfall rates at 0.01% have close attenuation values, while the attenuation values are different in stations with different point rainfall rates. This can be noticed in Minna and Makurdi that both recorded 75.5 mm/h at 0.01%. The computed attenuation by the ITU-R P.618-9 model is 13.5 dB for Minna and 13.8 dB for Makurdi. Jos station, with the same value of rain rate also recorded very close attenuation value of 12.0 dB. This trend is replicated by the Bryant and Garcia-Lopez models. Stations like Abuja and Anyigba that recorded lower point rainfall rates had lower rain attenuation computed by the models. The Simple attenuation and Svjatogor models underestimated the rain attenuation as predicted values deviated greatly from those of the other models. The attenuation values computed by the best performing models are further presented in Table 36.6 for clearer illustration.

It is clearly shown in Table 36.6 that these three models also predicted closely at the other time percentage exceedances of 0.001, 0.1 and 1%.

The cumulative distribution of predicted rain attenuation at 42.5° elevation angle are presented in Fig. 36.3a–e.

From Fig. 36.3, it is observed that predicted rain attenuation values are a bit higher at 42.5° elevation angle when compared with values obtained at 55°. The deviation in values between the two elevation angles is about 2–5 dB for the entire distribution. Again, values predicted by the Bryant and Garcia-Lopez models are close to the ITU-R P.618, while computed values from SAM and Svjatogor models are low.

Figure 36.4a–e show the cumulative distribution of predicted rain attenuation at 23° elevation angle

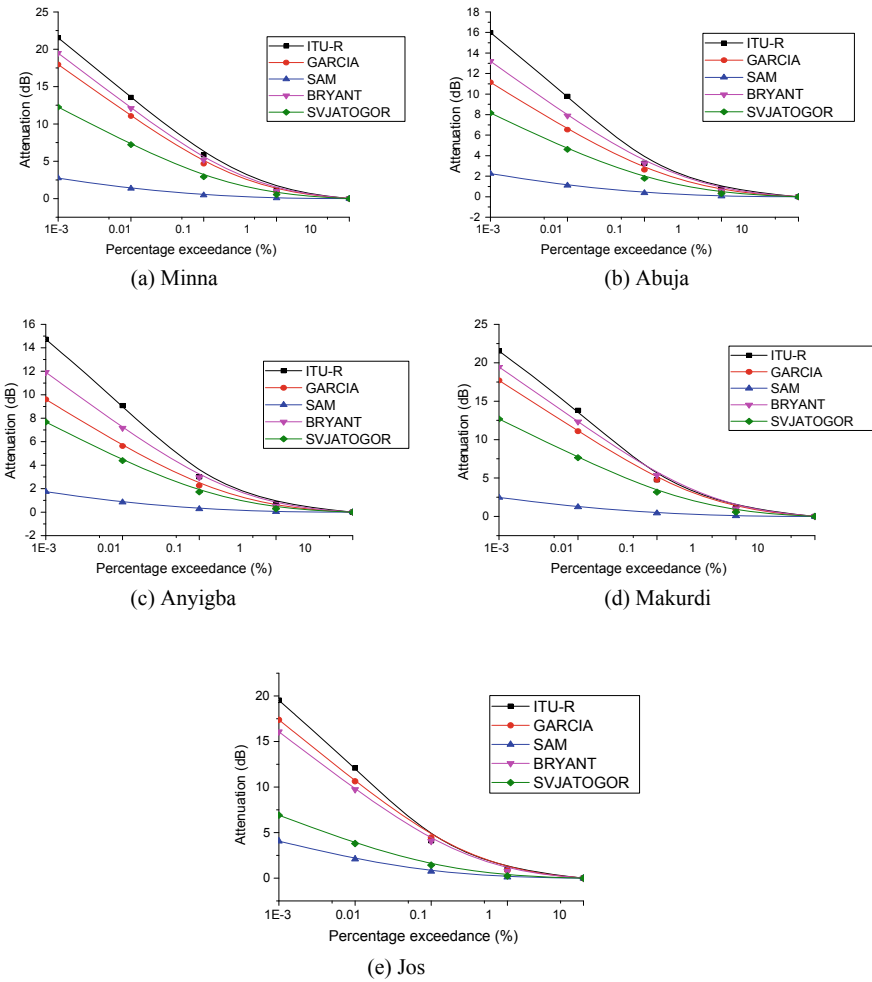


Fig. 36.2 Predicted attenuation at 55° elevation angle

From Fig. 36.4, It is observed that there is an increase in the computed attenuation values at 23° elevation angle. These higher values are due to the longer path length of the rain region associated with this lower angle. This implies that satellite-earth links propagating at this elevation angle will suffer more signal outage than those propagating at higher elevation angles.

Table 36.6 Predicted rain attenuation for the three best attenuation models

% Exceedance	Stations	ITU-R P.618-9 (dB)	Bryant (dB)	Garcia-Lopez (dB)
0.001	Minna	21.5	19.5	18.0
	Abuja	16.0	13.0	11.0
	Makurdi	21.5	19.5	18.0
	Anyigba	15.0	12.0	9.0
	Jos	19.5	16.0	17.0
0.01	Minna	13.5	12.0	11.0
	Abuja	10.0	8.0	6.5
	Makurdi	13.8	12.0	11.0
	Anyigba	9.0	7.0	5.6
	Jos	12.0	9.7	10.6
0.1	Minna	6.0	5.0	5.0
	Abuja	3.3	3.2	2.6
	Makurdi	5.0	5.0	5.0
	Anyigba	3.0	3.0	2.3
	Jos	4.0	4.0	4.5
1	Minna	1.1	1.0	0.9
	Abuja	0.8	0.6	0.5
	Makurdi	1.2	1.0	0.9
	Anyigba	0.7	0.5	0.4
	Jos	1.0	0.8	0.8

36.5 Conclusion

Rain attenuation predictions on satellite-earth links at Ku-band middle frequency operating at 55°, 42.5° and 23° elevation angles were made using five different rain attenuation models. For the computed rain attenuation, it has been shown that higher attenuation was experienced at lower percentage of time exceedance, while lower attenuation was experienced at higher percentage of time exceedance. Also, for the three elevation angles considered, rain attenuation was highest at 23°, followed by 42.5°, while 55° elevation angle had the lowest computed attenuation (though with slightly lower values than at 42.5°). This implies that higher attenuation is experienced at lower elevation angles, while lower attenuation is experienced at higher elevation angles. In all the stations, attenuation generally ranged from 6 to 14 dB at 55° elevation angle, 6 to 14 dB at 42.5° elevation angle and from 6 to 19 dB at 23° elevation angle at time percentage exceedance of 0.01% for models with close predictions.

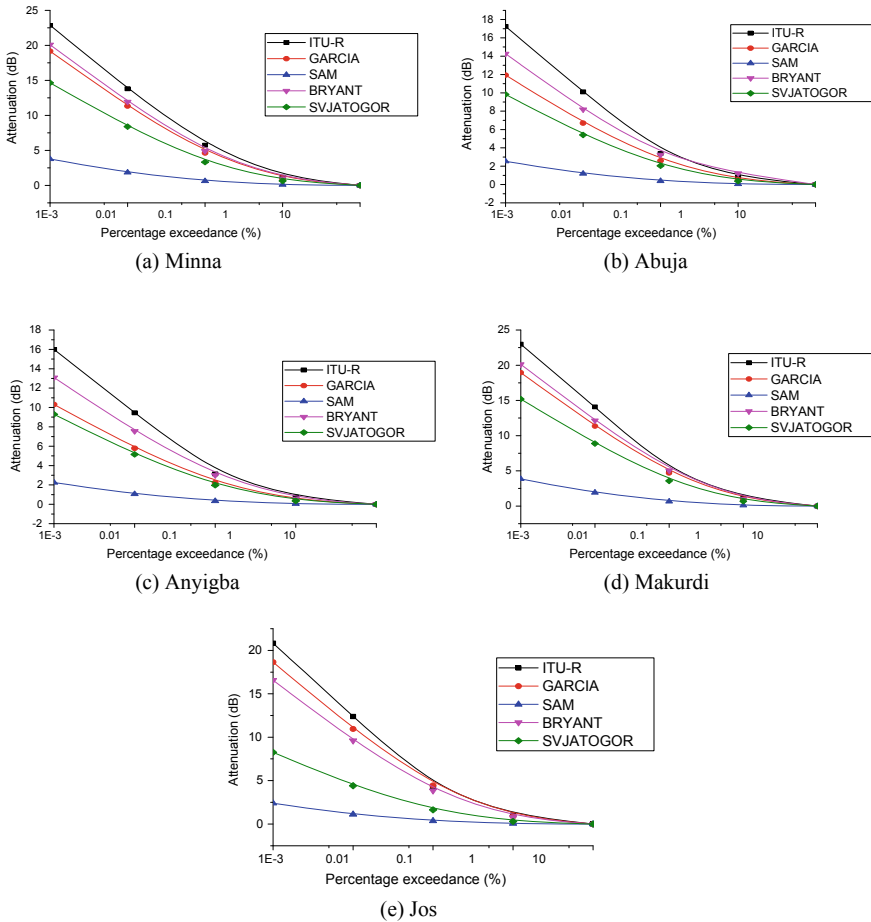


Fig. 36.3 Predicted attenuation at 42.5° elevation angle

In addition, results obtained have shown that three of the five models, the ITU-R P.618, Garcia-Lopez and Bryant were in good agreement, while predictions from the Simple attenuation and Svjatogor models underestimated the predicted rain attenuation values. Thus, the ITU-R P.618, Garcia-Lopez and Bryant models can be used to satisfactorily predict rain attenuation in North Central Nigeria.

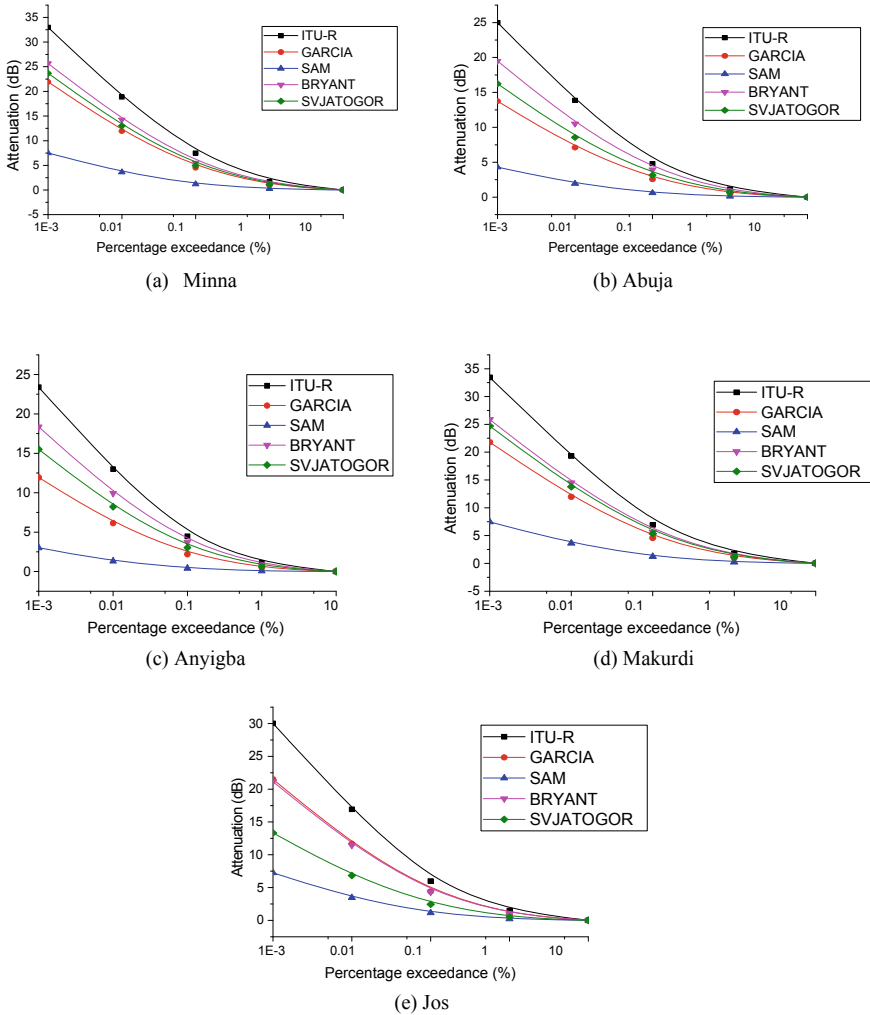


Fig. 36.4 Predicted attenuation at 23° elevation angle

Acknowledgements The author appreciates the Centre for atmospheric research, Anyigba, Nigeria for providing the rainfall measuring equipment used in this research.

References

1. R.K. Crane, Rain attenuation models: Attenuation by clouds and rain, in *Propagation handbook for wireless communication system design*. (CRC Press, USA, 2003), pp. 225–280
2. J.S. Mandeep, Comparison of rain rate models for equatorial climate in South East Asia. *Geofizika* **28**, 265–274 (2011)
3. S. Shrestha, J.J. Park, D.Y. Choi, Rain rate modeling of 1 min from various integration times in South Korea. *SpringerPlus* **5**(1), 1–34 (2016)
4. S. Shrestha, D.Y. Choi, Characterization of rain specific attenuation and frequency scaling method for satellite communication in South Korea. *Int. J. Antennas Propag.* **2017**, 1–16 (2017)
5. M.S. Hossain, M.A. Islam, Estimation of rain attenuation at EHF bands for earth-to-satellite links in Bangladesh. *International Conference on Electrical, Computer and Communication Engineering*, Cox's Bazar, Bangladesh, pp 589–593 (2017)
6. S. Shrestha, D.Y. Choi, Diurnal and monthly variations of rain rate and rain attenuation on Ka-band satellite communication in South Korea. *Prog. Electromag. Res.* **B 80**, 151–171 (2018)
7. L. Rong, A new method of uplink power compensation of rain attenuation of satellite communication system. *International Conference on Automation, Mechanical Control and Computational Engineering*, pp. 2181–2185 (2015)
8. M.P.M. Hall, *Effects of the troposphere on radio communication* (Peter Peregrinus Limited, U.K., 1979)
9. M. Tamosiunaite, M. Tamosiuniene, A. Gruodis, S. Tamosiunas, Prediction of electromagnetic wave attenuation due to water in the atmosphere. 1. Attenuation due to rain. *Innovative Infotechnologies Sci. Bus. Educ.* **2**(9), 3–10 (2010)
10. R. Oktaviani, Marzuki, Estimation of rainfall rate cumulative distribution in Indonesia using global satellite mapping of precipitation data. *International Conference on Basic Science and its Application*, pp. 259–265 (2019)
11. Y. Ng, M. Singh, J. Singh, V. Thiruchelvam, Performance analysis of 60-min to 1-min integration time rain rate conversion models in Malaysia. *J Atm and Solar-Terr Phys* **167**, 13–22 (2017)
12. S. Shrestha, D. Choi, Study of 1-min rain rate integration statistics in South Korea. *J Atm Solar-Terr. Phys.* (2017)
13. I. Rafiqul, M. Alam, A.K. Lwas, S.Y. Mohamad, Rain rate distributions for microwave link design based on long term measurement in Malaysia. *Indonesia J. Elect. Eng. Comp. Sci.* **10**(3), 1023–1029 (2018)
14. R. Singh, R. Acharya, Development of a new global model for estimating one-minute rainfall rate. *IEEE Trans Geosci Remote Sens* **56**(11), 6462–6468 (2019)
15. COST 225, Radiowave propagation modelling for SatCom services at Ku-band and above. Final report, European Space Agency, the Netherlands, pp. 74–97 (2002)
16. K.C. Igwe, O.D. Oyedum, M.O. Ajewole, A.M. Aibinu, Evaluation of some rain attenuation prediction models for satellite communication at Ku and Ka bands. *J. Atm. Solar-Terr Phys.* **188**, 52–61 (2019)
17. J. Lavergnat, P.A. Gole, Stochastic raindrop time distribution model. *J Appl Met* **37**, 805–818 (1998)
18. C. Ito, Y. Hosoya, *Proceedings of ISAP'04, Sendai, JAPAN*, pp. 1361–1364 (2004)
19. L.D. Emiliani, L. Luini, C. Capsoni, Analysis and parameterization of methodologies for the conversion of rain-rate cumulative distributions from various integration times to one minute. *IEEE Ant. Propag. Mag.* **51**(3), 70–80 (2009)
20. K.C. Igwe, O.D. Oyedum, M.O. Ajewole, A.M. Aibinu, J.A. Ezenwora, Performance evaluation of some rain rate conversion models for microwave propagation studies. *Adv. Space Res.* **67**, 3098–3105 (2021)
21. ITU-R, *Propagation data and prediction methods required for the design of earth-space telecommunication systems. Rec P 618-9* (International Telecommunication Union, Geneva, 2007)

22. G.H. Bryant, I. Adimula, C. Riva, G. Brussard, Rain attenuation statistics from rain column, diameters and heights. *Int. J. Sat. Commun.* **19**, 263–283 (1999)
23. W.L. Stutzman, W.K. Dishman, Correction to a simple model for the estimation of rain-induced attenuation along earth-space paths at millimeter wavelengths. *Rad. Sci.* **19**, 946 (1984)
24. J.A. Garcia-Lopez, J.M. Hernando, J. Selga, Simple rain attenuation method for satellite radio links. Year-to-year variability of rainfall for microwave applications in the USA. *IEEE Trans Ant Propag* **36**(3), 444–448 (1988)
25. L. Svjatogor, Prostranstvennaia korelacia vypadenjija dozdznej vdol zemnoj poverchnostji (in Russian), Symposium expertov stran uchastnic programmy. INTERKOSMOS (Interkosmos symposium, theme 5 of the established telecommunication working group, Dresden, GDR, 1985)
26. ITU-R, *Rain height model for prediction methods. Rec P 839-3* (International Telecommunication Union, Geneva, 2001)
27. ITU-R, *Specific attenuation model for rain for use in prediction methods. Rec P 838-3* (International Telecommunication Union, Geneva, 2005)
28. G. Immadi, S.K. Kotamraju, M.V. Narayana, H. Khan, G. Viswanath, I. Avinash, Measurement of rain attenuation for Ku band satellite signal in tropical environment using DAH, SAM models. *ARNP J. Eng. Appl. Sci.* **10**(4), 1717–1722 (2015)
29. Y.I.O. Abayomi, N.H.H. Khamis, Rain attenuation modelling and mitigation in the tropics: brief review. *Int. J. Elect. Comp. Eng.* **2**(6), 748–757 (2012)
30. Y.S. Choi, J.H. Lee, J.M. Kim, Rain attenuation measurements of the KoreaSat beacon signal on 12 GHz. CLIMPARA '98, Ottawa, Canada, pp. 208–211 (1997)
31. L.D. Emiliani, E. Agudelo, E. Gutierrez, J. Restrepo, C. Fradique-Mendez, Development of rain-attenuation and rain-rate maps for satellite system design in the Ku- and Ka-bands in Columbia *IEEE Ant. Propag. Mag.* **46**(6), 54–68 (2004)
32. J.S. Mandeep, J.E. Allnut, Rain attenuation predictions at Ku-band in South East Asia countries. *Prog. Electromag. Res. PIERS* **76**, 65–74 (2007)
33. P. Panchal, R. Joshi, Performance analysis and simulation of rain attenuation models at 12–40 GHz band for an earth space path over Indian cities. *7th International conference on Communication Computer Virtualization*, 79, pp. 801–808 (2016)